JOURNAL OF BACTERIOLOGY, July 2008, p. 4666–4676 Vol. 190, No. 13
0021-9193/08/$08.00+0 doi:10.1128/JB.00093-08

Mutagenesis of the *Shigella flexneri* Autotransporter IcsA Reveals Novel Functional Regions Involved in IcsA Biogenesis and Recruitment of Host Neural Wiscott-Aldrich Syndrome Protein▽†

Kerrie L. May and Renato Morona*

Australian Bacterial Pathogenesis Program, Discipline of Microbiology and Immunology, School of Molecular and Biomedical Science, University of Adelaide, South Australia, Australia

Received 17 January 2008/Accepted 28 April 2008

The IcsA (VirG) protein of *Shigella flexneri* is a polarly localized, outer membrane protein that is essential for virulence. Within host cells, IcsA activates the host actin regulatory protein, neural Wiskott-Aldrich syndrome protein (N-WASP), which in turn recruits the Arp2/3 complex, which nucleates host actin to form F-actin comet tails and initiate bacterial motility. Linker insertion mutagenesis was undertaken to randomly introduce 5-amino-acid in-frame insertions within IcsA. Forty-seven linker insertion mutants were isolated and expressed in *S. flexneri* Δ*icsA* strains. Mutants were characterized for IcsA protein production, cell surface expression and localization, intercellular spreading, F-actin comet tail formation, and N-WASP recruitment. Using this approach, we have identified a putative autochaperone region required for IcsA biogenesis, and our data suggest an additional region, not previously identified, is required for N-WASP recruitment.

Shigella flexneri causes bacillary dysentery in humans due to bacterial invasion and colonization of the colonic epithelium that leads to acute mucosal inflammation (42). *S. flexneri* IcsA (VirG), an essential virulence factor, is a polarly localized, outer membrane (OM) protein that is required for intra- and intercellular spreading throughout the host epithelium (17, 23, 24, 27, 45, 52). Within host cells, IcsA interacts with the host actin regulatory protein, neural Wiskott-Aldrich syndrome protein (N-WASP), which in turn recruits the host Arp2/3 complex, which polymerizes host globular actin into filamentous actin (F-actin) (10, 17, 41). The accumulation of F-actin in "comet tails" at one pole of the bacterium initiates bacterial actin-based motility (ABM) (2, 10, 17).

IcsA is an autotransporter (AT) protein, belonging to the largest family of gram-negative bacterial extracellular proteins, with more than 700 members (40). Like other members of this family, IcsA consists of three major domains: an N-terminal signal sequence (amino acids [aa] 1 to 52), to direct Sec-dependent protein transport across the inner-membrane; and a C-terminal translocation domain (aa 759 to 1102) that enables export of the remaining N-terminal region of IcsA, the passenger domain (aa 53 to 758), across the OM (5, 6, 19, 48). The passenger domain becomes exposed on the outer surface, anchored by the translocation domain, and is responsible for IcsA activity in N-WASP recruitment and ultimately bacterial motility (17, 52).

Within the host cell, N-WASP regulates the host actin cytoskeleton and functions as a link between signaling pathways and de novo actin polymerization, thereby initiating host cell motility and morphological changes (28, 55). $IcsA_{103-433}$, which contains a series of glycine-rich repeats (GRR) (aa 140 to 307), is sufficient for N-WASP binding in vitro (49, 50). However, in vitro actin polymerization requires aa 53 to 508, and it has been suggested that the residues involved in N-WASP recruitment in vivo are within this region (17, 51, 52). Correspondingly, a *Shigella* strain expressing $IcsA_{\Delta 509-729}$ was reported to recruit N-WASP inside host cells (49). However, this mutant had previously been shown to have a defect in F-actin tail formation, which was attributed to nonpolar IcsA localization (51). Consequently, whether aa 53 to 508 of IcsA are actually sufficient for F-actin comet tail formation inside host cells awaits clear verification. A region encompassing the GRR region (aa 104 to 506) has been shown to interact with the host protein vinculin (51), and another region (aa 320 to 433) interacts with *S. flexneri* IcsB and the host autophagy protein, Atg5 (37).

Two regions of the IcsA passenger domain, polar localization region 1 (aa 1 to 104) and polar localization region 2 (aa 507 to 620), have been shown to be independently responsible for targeting IcsA export to the old cell pole (9, 51). IcsA polarity is thought to enhance unidirectional movement of the bacteria, which has been shown to correlate with an increased frequency of protrusion formation into adjacent host cells (a process that leads to intercellular spreading) (29). Additionally, a cleavage site for the virulence plasmid-encoded, OM, serine protease IcsP (SopA), exists between residues R_{758} and R_{759}. Cleavage of IcsA by IcsP results in the release of the 95-kDa N-terminal fragment into the extracellular milieu at a low efficiency, such that during exponential growth of the bacteria, 80% of the IcsA molecules remain uncleaved and anchored to the OM (11, 13, 15, 46, 47). The significance of IcsA cleavage by IcsP remains controversial, although it has been suggested that it functions to enhance IcsA polarity (13, 46).

Previous IcsA structure and function studies have relied predominantly on relatively large deletion mutations of IcsA regions (8, 49–51). Such approaches may have resulted in the

* Corresponding author. Mailing address: School of Molecular and Biomedical Science, University of Adelaide, South Australia 5005, Australia. Phone: 61-8-83034151. Fax: 61-8-83037532. E-mail: renato.morona@adelaide.edu.au.

† Supplemental material for this article may be found at http://jb.asm.org/.

▽ Published ahead of print on 2 May 2008.

TABLE 1. Bacterial strains and plasmids

Strain or plasmid	Relevant characteristics[a]	Reference or source
E. coli K-12		
DH5α	Cloning host	Gibco-BRL
UT5600	Protease-deficient strain; Δ*ompT* Δ*ompP*; Sm^r	Laboratory stock
S. flexneri		
2457T	*S. flexneri* 2a WT	53
RMA2041	2457T Δ*icsA*::Tc^r	54
RMA2090	RMA2041(pIcsA)	54
RMA2043	RMA2041 Δ*rmlD*::Km^r	54
RMA2107	RMA2043(pIcsA)	54
Plasmids		
pIcsA	*icsA* gene cloned into pBR322; Ap^r; medium copy no.; ColE1 *ori*	33
pD10	Plasmid encoding $IcsA_{WT}$; Tp^r	51
pD10-*virG*1	Plasmid encoding $IcsA_{\Delta 103–320}$; Tp^r	51
pD10-*virG*3	Plasmid encoding $IcsA_{\Delta 508–730}$; Tp^r	51
pD10-*virG*4	Plasmid encoding $IcsA_{\Delta 103–507}$; Tp^r	51

[a] Sm^r, streptomycin resistant; Tc^r, tetracyline resistant; Km^r, kanamycin resistant; Ap^r, ampicillin resistant; Tp^r, trimethroprim resistant.

removal of multiple functional domains, complicating the interpretation of the phenotypes of the *icsA* mutants in those studies. In previous studies we have provided evidence of masking of IcsA function by lipopolysaccharide O antigen (LPS Oag) (31, 32). LPS is a major constituent of the OM of gram-negative bacteria, consisting of a lipid A, a core polysaccharide component, and an Oag polysaccharide chain (also called O antigen) that extends into the extracellular milieu (4, 21). Hypothetically, truncated IcsA proteins may be more prone to LPS Oag masking, further complicating the assessment of their activity. To better understand the IcsA structure-function relationship, pentapeptide linker insertion mutagenesis of IcsA was undertaken and 47 unique $IcsA_i$ mutants were isolated and characterized. In addition to evaluating the abilities of various $IcsA_i$ mutants to interact with N-WASP in the presence of native LPS-Oag, we also investigated the influence of LPS Oag on IcsA–N-WASP interactions by assessing the function of these proteins in the absence of LPS Oag. We have identified regions of IcsA required for N-WASP recruitment inside host cells and a putative autochaperone region required for IcsA biogenesis.

MATERIALS AND METHODS

Bacterial strains and plasmids. The strains and plasmids used in this study are listed in Table 1.

Growth media and growth conditions. *S. flexneri* strains were grown from a Congo red-positive colony. All bacterial strains were routinely cultured in Luria Bertani (LB). Bacteria were grown in media with antibiotics for 16 h with aeration and then subcultured 1:50 and grown to log phase by incubation with aeration for 2 h at 37°C. Where appropriate, media were supplemented with ampicillin (100 μg/ml), chloramphenicol (25 μg/ml), kanamycin (50 μg/ml), tetracycline (50 μg/ml), or trimethroprim (10 μg/ml).

DNA methods. *Escherichia coli* K-12 strain DH5α was used for routine cloning, and general cloning techniques and PCR and DNA sequencing were performed as described previously (1, 34).

Antibodies and antisera. Affinity-purified rabbit polyclonal anti-IcsA antiserum was produced in our laboratory as described previously (53). The polyclonal rabbit anti-N-WASP antibody was initially a generous gift from Hiroaki Miki. Subsequent stocks of comparable polyclonal rabbit anti-N-WASP antibodies were made in our laboratory according to the method described by Fukuoka et al. (16). The vector encoding a glutathione *S*-transferase-tagged carboxyl-terminal region of N-WASP (VCA region; amino acids 388 to 501), used to produce purified protein for the production of antiserum, was kindly provided by Hiroaki Miki. The anti-N-WASP antibody was used at 1:100. The polyclonal anti-*Shigella* LPS (3, 4) was from Denka Seiken Co. (Japan) and was used at 1:100.

Linker insertion mutagenesis using the Mutation Generation System (Finnzymes). Linker insertion mutagenesis of IcsA was performed using the Mutation Generation System (Finnzymes) according to the manufacturer's instructions. Briefly, an in vitro transposition reaction was carried out to randomly introduce an artificial entranceposon (M1-Cm^r) into pIcsA (33, 54), which encodes wild-type (WT) IcsA ($IcsA_{WT}$). The entranceposons were removed from the mutated plasmids using the NotI restriction enzyme, and the digested plasmids were then religated to leave an in-frame insertion of 15 bp encoding 5 aa. Plasmids were screened initially by PCR using the NotI miniprimer (Finnzymes) (a primer complementary to 10 bp of the insertion) and primer 2156IcsAF (see Table S2 in the supplemental material), which is complementary to a region 100 bp upstream of the *icsA* gene in pIcsA, to identify those which contained insertions within the IcsA passenger domain. The location of each insertion and the encoded amino acids for each of these plasmids were determined by DNA sequencing using primers 2156IcsAF, IcsA549F, IcsA2381R, 2170IcsAR (see Table S2 in the supplemental material).

Preparation of whole-cell lysates. The equivalent of 5×10^8 bacteria were pelleted by centrifugation ($3{,}300 \times g$ for 6 min at 4°C and resuspended in 100 μl of 2× sample buffer (26).

TCA precipitation of culture supernatants. The equivalent of 5×10^9 bacteria were pelleted by centrifugation at $2{,}200 \times g$ for 10 min at 4°C. The supernatants were collected, supplemented with 5% ice-cold trichloroacetic acid (TCA), and incubated on ice for 1 h. The TCA precipitate was pelleted by centrifugation at $40\,000 \times g$ for 30 min at 4°C. The supernatant was removed and the pellet centrifuged again for 5 min as before to remove the remaining supernatant. The protein pellet was washed with ice-cold acetone and centrifuged for another 5 min and the acetone carefully removed. The pellet was air-dried and then resuspended in 100 μl of 1× sample buffer (26).

Western transfer and detection. Proteins were separated on 7.5% or 12% sodium dodecyl sulfate-polyacrylamide gel electrophoresis (SDS-PAGE) gels and transferred to a nitrocellulose membrane. The membrane was blocked for 1 h in TTBS (Tris-buffered saline, 0.05% Tween 20) containing 5% skim milk and incubated with the desired primary antibody in the same buffer overnight. After three 10-min washes in TTBS, the membrane was incubated with horseradish peroxidase-conjugated goat antirabbit or a horseradish peroxidase-conjugated goat antimouse secondary antibodies (Biomediq DPC) for 2 h and washed three times in TTBS and then three times in Tris-buffered saline. The membrane was incubated with chemiluminescence blotting substrate (Roche) for 1 min. Chemiluminescence was detected by exposure of the membrane to X-ray film (Agfa), and the film was developed using a Curix 60 automatic X-ray film processor (Agfa).

Indirect immunofluorescence (IF) of whole bacteria. Log-phase bacteria were pelleted by centrifugation ($2{,}200 \times g$, 10 min, 4°C) and the supernatant discarded. Bacteria were fixed in formalin (3.7% paraformaldehyde in 0.85% saline) for 15 min at room temperature. Sterile coverslips were placed in 24-well trays and incubated with 10% poly-L-lysine in phosphate-buffered saline (PBS) for 1 min. The poly-L-lysine was aspirated, and formalin fixed bacteria were centrifuged onto poly-L-lysine-coated coverslips at $1{,}000 \times g$ for 5 min. Bacteria were incubated with the desired primary antibody diluted 1:100 in PBS with 10% fetal calf serum (FCS). Bacteria were washed three times in PBS and incubated with either Alexa 488-conjugated donkey antirabbit or Alexa 488-conjugated donkey antimouse secondary antibodies (Molecular Probes) diluted 1:100 in PBS with 10% FCS.

Plaque assays. Plaque assays were performed with HeLa cells using a modification of the method described by Oaks et al. (35). HeLa cells were seeded to 60-mm-diameter, six-well trays at 1×10^6 in minimal essential medium–10% FCS with penicillin and streptomycin. Cells were grown to confluence overnight and washed twice with Dulbecco's PBS (D-PBS) and once in Dulbecco's modified Eagle medium (DMEM) prior to inoculation. Log-phase bacteria were diluted to 1:100 and 1:300 in DMEM, and 0.2 ml was added to each well. Trays were incubated at 37°C in a humidified CO_2 (5%) incubator, and the trays were rocked gently every 15 min to ensure that the inoculum was spread evenly across

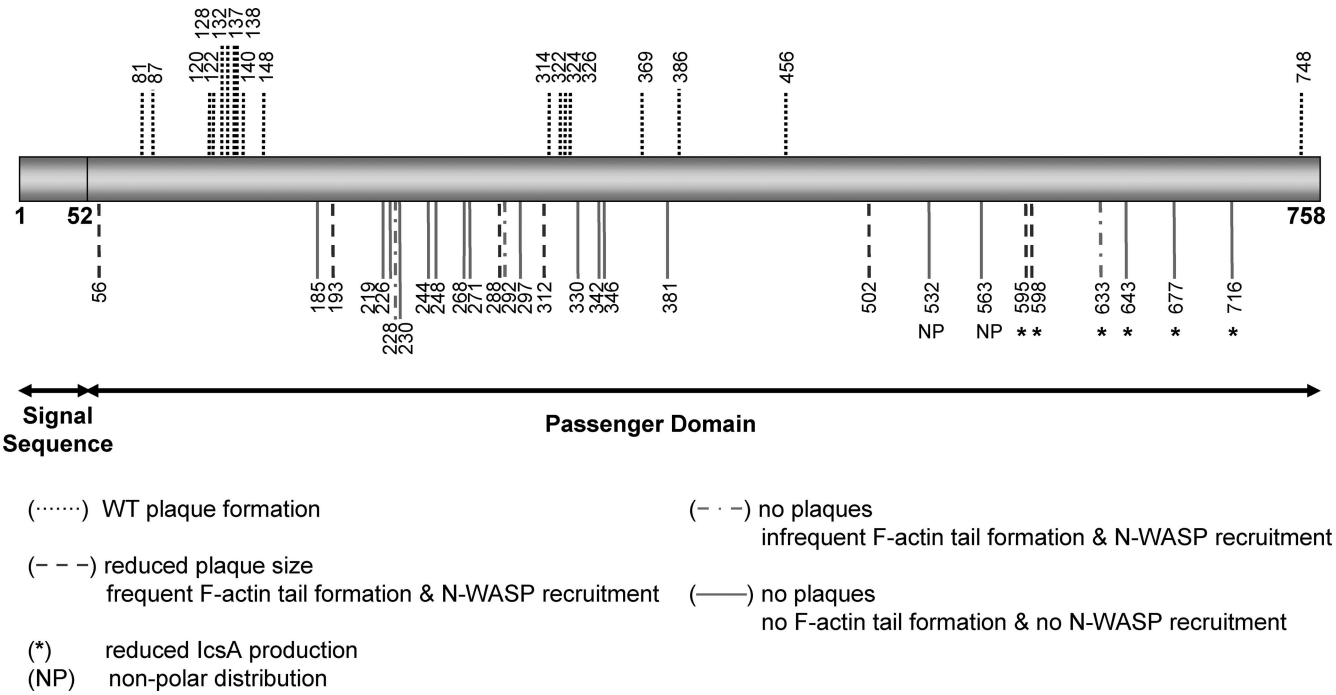

FIG. 1. Schematic locations of the 5 amino acid insertions in 47 mutant $IcsA_i$ proteins and the corresponding phenotypes. The location of the linker insertion for each of the 47 $IcsA_i$ mutants is indicated with a vertical line.

the monolayer. At 90 min postinfection, the inoculum was carefully aspirated and 4 ml of the first overlay (DMEM, 5% FCS, 20 μg/ml of gentamicin, 0.5% agarose [Seakem ME]) was added to each well. The second overlay (DMEM, 5% FCS, 20 μg/ml of gentamicin, 0.5% agarose, 0.1% Neutral Red solution [Gibco BRL]) was added at either 24 h or 48 h postinfection and plaque formation observed 6 to 8 h later. Plaques were in general visible without staining at 48 h.

Trypsin accessibility assay. Limited proteolysis was performed as described by Oliver et al. (39) with modifications. The equivalent of 5×10^9 log-phase bacteria were pelleted by centrifugation, the supernatant was discarded, and the pellet was resuspended in 150 μl of PBS. Bacterial suspensions were supplemented with 0.1 μg/ml of Trypsin from bovine pancreas (no. 109819; Roche) and incubated at room temperature to allow proteolysis. Aliquots were taken at several time points (0 min, 5 min, and 10 min) and supplemented with 1 mM phenylmethylsulphonylfluoride (Sigma) to inhibit Trypsin and further proteolysis. An equal volume of 2× sample buffer (26) was added to each sample, all of which were then heated at 100°C for 5 min prior to SDS-PAGE and western immunoblotting.

Infection of tissue culture monolayers with *S. flexneri* and IF labeling. Infection of tissue culture cells and IF staining were performed as recently described (31). Briefly, 5×10^8 log-phase bacteria were pelleted by centrifugation (3,300 × *g*, 6 min) and resuspended at 10^9 bacteria/ml in D-PBS. One hundred microliters of bacterial suspension was then centrifuged onto HeLa cells grown to semiconfluence on sterile glass coverslips. After 1 h of incubation at 37°C in 5% CO_2, the infected cells were washed three times with D-PBS and incubated with 0.5 ml minimal essential medium containing 40 μg/ml of gentamicin for a further 1.5 h. Infected cells were washed a further three times in D-PBS and then fixed for 15 min in formalin, incubated with 50 mM NH_4Cl in D-PBS for 10 min, and then permeabilized with 0.1% Triton X-100 in H_2O for 5 min. After blocking in 10% FCS in PBS, the infected cells were incubated at 37°C for 30 min with the desired primary antibody. After washing in PBS, coverslips were incubated with either Alexa 594-conjugated donkey antirabbit or Alexa 594-conjugated donkey antimouse secondary antibodies (Molecular probes) (1:100), as required. F-actin was visualized by staining with fluorescein isothiocyanate (FITC) phalloidin (0.1 μg/ml; Sigma), and 4′,6′-diamidino-2-phenylindole (DAPI) (0.1 μg/ml, Sigma) was used to counterstain bacteria and cellular nuclei as required.

Microscopy. Coverslips were mounted on glass slides with Mowiol 4-88 (Calbiochem) containing 20 μg/ml *p*-phenylenediamine (Sigma) and examined with an Olympus IX-70 microscope with phase-contrast optics using a 100× oil immersion objective and a 1.5× enlarger as required. Fluorescence and phase-contrast images were false color merged using the Metamorph software program (version 6.3r7; Molecular Devices).

Quantitation of F-actin tail formation and N-WASP recruitment. Quantification of F-actin comet tails is made difficult by the fact that their numbers naturally vary greatly between cells. Therefore, the quantitation method used by Frischknecht et al. (14) was adopted, in which the presence of a single actin tail within an infected cell is scored as positive. N-WASP recruitment was also quantitated in this manner. Initially, for each strain, 20 cells were observed and scored as described above in two independent experiments. For strains expressing the mutant $IcsA_{i56}$, $IcsA_{i193}$, $IcsA_{i288}$, $IcsA_{i312}$, or $IcsA_{i502}$, where the frequency of F-actin tail formation was comparable to that of the WT despite obvious intercellular spreading defects, 100 cells were scored in three independent experiments.

RESULTS

Linker insertion mutagenesis of IcsA passenger domain. Pentapeptide linker insertion mutagenesis of IcsA was performed using the Mutation Generation System (Finnzymes) as described in Materials and Methods. Forty-seven plasmids were obtained that harbored unique insertions within the IcsA passenger domain (Fig. 1; also see Table S1 in the supplemental material). Plasmid pIcsA and those encoding the IcsA linker insertion mutants ($IcsA_i$) were electroporated into an *S. flexneri* Δ*icsA* strain (RMA2041; Table 1) to enable characterization of $IcsA_i$ production and function.

Effects of linker insertions on IcsA production and secretion. To investigate the effects on protein production arising from the 5-aa linker insertion in each $IcsA_i$ mutant, SDS-PAGE and Western immunoblotting with IcsA antibody were performed on whole-cell lysates. In 41 of 47 mutants, IcsA protein levels were comparable to those of the WT (Table 2). The mutant proteins $IcsA_{i595}$, $IcsA_{i598}$, $IcsA_{i633}$, $IcsA_{i643}$, $IcsA_{i677}$, and $IcsA_{i716}$ demonstrated aberrant production in *S.*

TABLE 2. Phenotypes of *S. flexneri* strains expressing $IcsA_i$ mutants

Protein[a]	$IcsA_i$ production[b]	$IcsA_i$ localization[c]	Plaque formation[d]	N-WASP recruitment[e]	F-actin tails[f]
$IcsA_{WT}$	+++	P	+++	+++	+++
$IcsA_{i56}$	**+++**	**P**	**++**	**+++**	**+++**
$IcsA_{i81}$	+++	P	+++	NT	NT
$IcsA_{i87}$	+++	P	+++	NT	NT
$IcsA_{i120}$	+++	P	+++	NT	NT
$IcsA_{i122}$	+++	P	+++	NT	NT
$IcsA_{i128}$	+++	P	+++	NT	NT
$IcsA_{i132}$	+++	P	+++	NT	NT
$IcsA_{i137}$	+++	P	+++	NT	NT
$IcsA_{i138}$	+++	P	+++	NT	NT
$IcsA_{i140}$	+++	P	+++	NT	NT
$IcsA_{i148}$	+++	P	+++	NT	NT
$IcsA_{i185}$	**+++**	**P**	**−**	**−**	**−**
$IcsA_{i193}$	**+++**	**P**	**+**	**+++**	**+++**
$IcsA_{i219}$	**+++**	**P**	**−**	**−**	**−**
$IcsA_{i226}$	**+++**	**P**	**−**	**−**	**−**
$IcsA_{i228}$	**+++**	**P**	**−**	**−**	**+**
$IcsA_{i230}$	**+++**	**P**	**−**	**−**	**−**
$IcsA_{i244}$	**+++**	**P**	**−**	**−**	**−**
$IcsA_{i248}$	**+++**	**P**	**−**	**−**	**−**
$IcsA_{i268}$	**+++**	**P**	**−**	**−**	**−**
$IcsA_{i271}$	**+++**	**P**	**−**	**−**	**−**
$IcsA_{i288}$	**+++**	**P**	**+**	**++**	**++**
$IcsA_{i292}$	**+++**	**P**	**−**	**+**	**+/−**
$IcsA_{i297}$	**+++**	**P**	**−**	**−**	**−**
$IcsA_{i312}$	**+++**	**P**	**+**	**+++**	**++**
$IcsA_{i314}$	+++	P	+++	NT	NT
$IcsA_{i322}$	+++	P	+++	NT	NT
$IcsA_{i324}$	+++	P	+++	NT	NT
$IcsA_{i326}$	+++	P	+++	NT	NT
$IcsA_{i330a}$	**+++**	**P**	**−**	**−**	**−**
$IcsA_{i330b}$	**+++**	**P**	**−**	**−**	**−**
$IcsA_{i342}$	**+++**	**P**	**−**	**−**	**−**
$IcsA_{i346}$	**+++**	**P**	**−**	**−**	**+/−**
$IcsA_{i369}$	+++	P	+++	NT	NT
$IcsA_{i381}$	**+++**	**P**	**−**	**−**	**−**
$IcsA_{i386}$	+++	P	+++	NT	NT
$IcsA_{i456}$	+++	P	+++	NT	NT
$IcsA_{i502}$	**+++**	**P**	**+**	**++**	**++**
$IcsA_{i532}$	**+++**	**NP**	**−**	**−**	**−**
$IcsA_{i563}$	**+++**	**NP**	**−**	**−**	**−**
$IcsA_{i595}$	**++**	**P**	**++**	**+++**	**+++**
$IcsA_{i598}$	**++**	**P**	**++**	**+++**	**+++**
$IcsA_{i633}$	**+**	**NT**	**−**	**+**	**+**
$IcsA_{i643}$	**+**	**NT**	**−**	**−**	**−**
$IcsA_{i677}$	**+**	**NT**	**−**	**−**	**−**
$IcsA_{i716}$	**+**	**NT**	**−**	**−**	**−**
$IcsA_{i748}$	+++	P	+++	NT	NT

[a] Mutants with altered function are in boldface, and mutants with WT function are in plain type.

[b] The "+++," "++," and "+" symbols indicate relative band intensities of Western immunoblots of whole-cell lysates.

[c] NP, nonpolar; P, polar.

[d] +++, WT plaques; ++, small plaques; +, foci; −, no plaques.

[e,f] +++, WT N-WASP recruitment/F-actin comet tail formation; ++, 20 to 90% reduction in N-WASP recruitment/F-actin tail formation relative to WT; +, >90% reduction in N-WASP recruitment/F-actin tail formation; +/−, F-actin capping; −, N-WASP/F-actin tail formation not detected; NT, not tested. Quantitated as detailed in Materials and Methods.

flexneri compared to that of $IcsA_{WT}$. The mutants $IcsA_{i595}$ and $IcsA_{i598}$ were produced at very low levels compared to $IcsA_{WT}$ (Fig. 2A), while $IcsA_{i633}$, $IcsA_{i643}$, $IcsA_{i677}$, and $IcsA_{i716}$ could be detected only with higher concentrations of anti-IcsA antibody (data not shown). For these mutants, along with $IcsA_{i595}$ and $IcsA_{i598}$, the amount of protein in the culture supernatant was also evaluated to determine if reduction of the full-length, OM forms of these proteins was possibly due to increased cleavage and secretion of these proteins into the supernatant. Cleaved forms of $IcsA_{i595}$ and $IcsA_{i598}$ were observed in the supernatant, although at lower levels than $IcsA_{WT}$, and the cleaved forms of $IcsA_{i633}$, $IcsA_{i643}$, $IcsA_{i677}$, and $IcsA_{i716}$ could not be detected (Fig. 2B). Notably, all six mutants possessed insertions immediately upstream of, or within, a region of IcsA (aa 634 to 735) that shares similarity to the putative autochaperone domain of the *Bordetella pertussis* BrkA autotransporter (39). Deletion of this region in BrkA made the protein susceptible to degradation by OM proteases and trypsin (39). Therefore, we expressed $IcsA_{i595}$, $IcsA_{i598}$, $IcsA_{i633}$, $IcsA_{i643}$, $IcsA_{i677}$, and $IcsA_{i716}$ in *E. coli* strain UT5600 (Table 1), which is deficient in the OM proteases *ompT* and *ompP*, to determine if production of these mutants could be restored. Mutants $IcsA_{i595}$, $IcsA_{i598}$, and $IcsA_{i633}$ were produced at levels comparable to $IcsA_{WT}$ in *E. coli* strain UT5600 (Fig. 2C). However, production of $IcsA_{i643}$, $IcsA_{i677}$, and $IcsA_{i716}$ was still greatly reduced in this background (Fig. 2C).

Trypsin accessibility of $IcsA_i$ mutants. Despite linker insertions being small (5 aa) and in-frame, these mutations could potentially disrupt the overall conformation of the protein, and this may account for the loss of function demonstrated by some $IcsA_i$ mutants. In order to evaluate this possibility, in situ limited proteolysis with trypsin was performed on 22 $IcsA_i$ mutants that were, as detailed later, negative for plaque for-

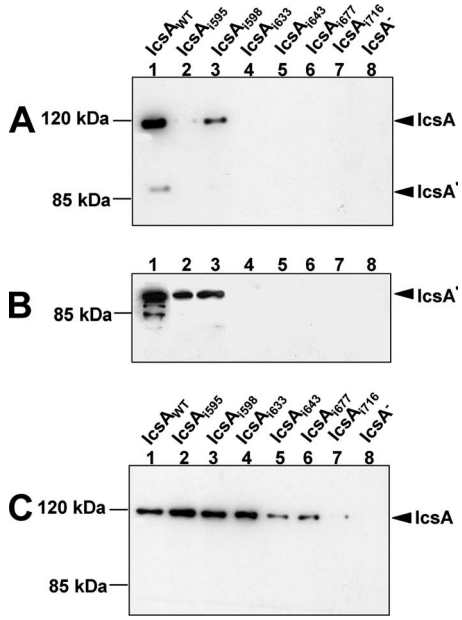

FIG. 2. Western blot analyses of $IcsA_i$ mutant production and secretion. (A) Whole-cell lysates from log-phase *S. flexneri* Δ*icsA* strains expressing $IcsA_{WT}$ or $IcsA_i$ mutants. (B) Tricholoroacetic acid-precipitated culture supernatants from log-phase *S. flexneri* Δ*icsA* strains expressing $IcsA_{WT}$ or $IcsA_i$ mutants. (C) Whole-cell lysates from *E. coli* UT5600 strains expressing $IcsA_{WT}$ or $IcsA_i$ mutants. All samples were electrophoresed on a 7.5% SDS-PAGE gel prior to Western blot analysis with anti-IcsA antibodies. The 116-kDa band corresponds to full-length IcsA, and the 95-kDa band corresponds to the cleaved form (IcsA′). Samples represent 1×10^8 cells or the culture supernatant equivalent of 1×10^9 cells.

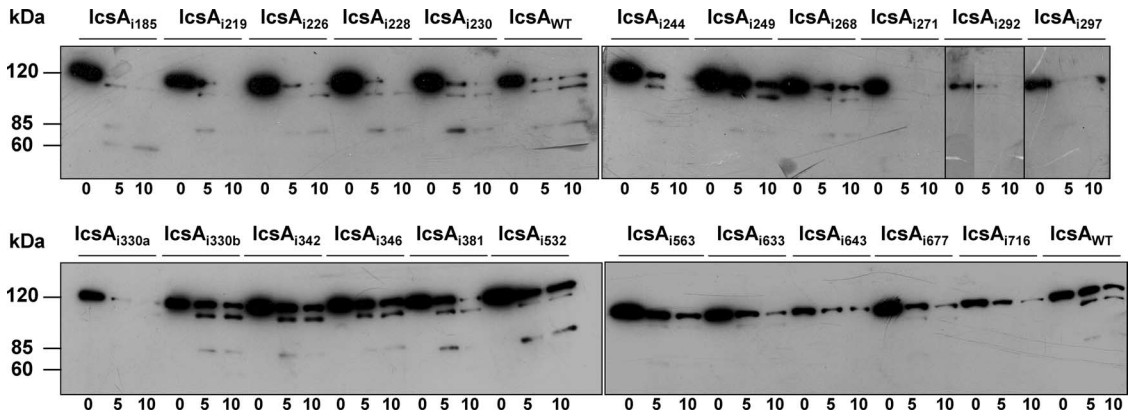

FIG. 3. Trypsin accessibility of IcsA$_i$ mutants. Log-phase cultures of *E. coli* UT5600 expressing IcsA$_{WT}$ or IcsA$_i$ mutants were treated with 0.1 μg/ml of trypsin at 25°C. Aliquots were taken at 0 min, 5 min, and 10 min and supplemented with 1 mM phenylmethylsulphonylfluoride to inhibit further proteolysis. Whole-cell lysates were electrophoresed on a 7.5% SDS-PAGE gel and subjected to Western blot analysis with anti-IcsA antibody. Samples represent the equivalent of 1×10^9 cells.

mation on a tissue culture monolayer (Table 2). To avoid intrinsic protein degradation by endogenous proteases, these studies were performed in an *E. coli* OM protease-deficient background (UT5600; Table 1). The protease digestion profiles of IcsA$_{WT}$ and 22 IcsA$_i$ mutants were compared after SDS-PAGE and Western immunoblotting with polyclonal anti-IcsA antibody. Major alterations to the protein conformation were expected to alter the accessibility of trypsin to sites within IcsA, thereby altering the profile of tryptic fragments. When the IcsA$_{WT}$ protein was subjected to in situ proteolysis with trypsin for either 5 or 10 min (Fig. 3), although band intensities varied between blots, three molecular mass bands of approximately 120 kDa, 100 kDa, and 85 kDa were consistently observed. The mutants IcsA$_{i185}$, IcsA$_{i219}$, IcsA$_{i228}$, IcsA$_{i244}$, IcsA$_{i271}$, IcsA$_{i292}$, IcsA$_{i297}$, IcsA$_{i330a}$, IcsA$_{i563}$, IcsA$_{i633}$, IcsA$_{i643}$, IcsA$_{i677}$, and IcsA$_{i716}$ had a proteolysis profile different from that of IcsA$_{WT}$, indicative of an altered sensitivity to trypsin. The latter suggests that these IcsA$_i$ mutant proteins have an altered conformation and interpretation of their phenotypes should be considered cautiously. Notably, five of these mutants (IcsA$_{i633}$, IcsA$_{i643}$, IcsA$_{i677}$, and IcsA$_{i716}$) possessed linker insertions within the putative autochaperone region. The mutants IcsA$_{i226}$, IcsA$_{i230}$, IcsA$_{i248}$, IcsA$_{i268}$, IcsA$_{i330b}$, IcsA$_{i342}$, IcsA$_{i346}$, IcsA$_{i381}$, and IcsA$_{i532}$ had proteolysis profiles comparable to that of IcsA$_{WT}$, signifying that they were likely to have a native conformation (Fig. 3). Hence, the corresponding phenotypes exhibited by *S. flexneri* expressing these proteins were unlikely to have resulted from major conformational changes. Interestingly, the mutants IcsA$_{i330a}$ and IcsA$_{i330b}$ had different proteolysis profiles despite harboring linker insertions in the same position. These mutants differed only in the encoded 5-aa insertion, with IcsA$_{i330a}$ harboring the insertion "TAAAI" and IcsA$_{i330b}$ the insertion "GAAAT" (see Table S1 in the supplemental material). However, these mutants did not differ phenotypically in any of the other functional assays.

Effect of linker insertions on IcsA surface expression and polar distribution. In order to assess the impact of each linker insertion on IcsA expression and distribution on the surface of bacteria, *S. flexneri* Δ*icsA* strains expressing IcsA$_i$ were examined by IF microscopy with anti-IcsA antibody. Of the six mutants that demonstrated reduced production by Western immunoblotting, IcsA$_{i633}$, IcsA$_{i643}$, IcsA$_{i677}$, and IcsA$_{i716}$ could not be detected on the surface of bacteria while IcsA$_{i595}$ and IcsA$_{i598}$ could be detected only weakly (Table 2). The remaining 41 IcsA$_i$ mutants could all be readily detected on the surface of *S. flexneri* (Table 2).

Thirty-nine IcsA$_i$ mutants that had WT production levels exhibited a surface distribution that was comparable to that of IcsA$_{WT}$, with these proteins being predominantly localized to the pole(s) and little or no protein detected on the lateral regions of bacteria. However, two mutants, IcsA$_{i532}$ and IcsA$_{i563}$, displayed altered localization (Fig. 4; Table 2). IcsA$_{i532}$ was distributed polarly on only 5% of bacteria, while for the majority of bacteria this protein was either distributed uniformly on the surface (47.5%) or distributed over the entire surface of the bacteria with some polar reinforcement (47.5%) (see Table S3 in the supplemental material). Similarly, the IcsA$_{i563}$ mutant was distributed polarly on only 22.5% of the bacteria, while for the majority of bacteria this protein was either distributed uniformly on the surface (35%) or distributed over the entire surface of the bacteria with some polar reinforcement (42.5%) (see Table S3 in the supplemental material). Notably, mutants with linker insertions in polar localization region 1 (aa 1 to 104) (IcsA$_{i56}$, IcsA$_{i81}$, and IcsA$_{i87}$) were all polarly distributed on at least 90% of bacteria (see Table S3 in the supplemental material). IcsA$_{i595}$ and IcsA$_{i598}$, which have a linker insertion in polar region 2, appeared to be polarly distributed (data not shown), but the percentage of bacteria with polar distribution could not be determined since the low level of expression of these proteins on the bacterial surface prevented reliable quantitation.

Effect of linker insertions on IcsA function in intercellular spreading. The ability of each IcsA$_i$ protein to support ABM was investigated by observing the capacity of *S. flexneri* Δ*icsA* strains expressing the mutated proteins to form plaques on HeLa cell monolayers. Plaque formation is an indication of intercellular spreading, a process that requires IcsA-dependent ABM. Eighteen of the *S. flexneri* strains expressing IcsA$_i$ proteins formed WT plaques (Table 2), indicating that linker insertions in these IcsA$_i$ mutants were located in functionally

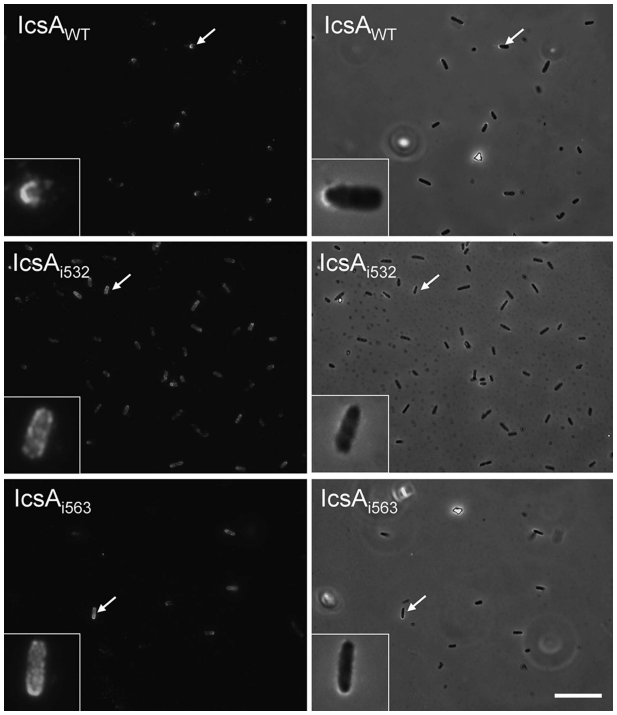

FIG. 4. Nonpolar distribution of IcsA$_{i532}$ and IcsA$_{i563}$ mutants on the surface of *S. flexneri*. IF microscopy of IcsA surface distribution. Log-phase cultures of *S. flexneri* strains expressing either IcsA$_{WT}$ or IcsA$_i$ were formalin fixed and labeled with anti-IcsA antibodies and Alexa 488-conjugated goat antirabbit secondary antibodies. For clarity, the IF image for each strain is accompanied by an overlay of the IF image with the corresponding phase-contrast image. Bar = 10 μm.

permissive sites. Twenty-two of the *S. flexneri* strains were unable to form plaques in three independent experiments (Table 2). These strains expressed IcsA$_i$ mutants with linker insertions either within the "GRR" region (aa 140 to 307) (IcsA$_{i185}$, IcsA$_{i219}$, IcsA$_{i226}$, IcsA$_{i228}$, IcsA$_{i230}$, IcsA$_{i244}$, IcsA$_{i248}$, IcsA$_{i268}$, IcsA$_{i271}$, IcsA$_{i292}$, and IcsA$_{i297}$), the IcsB binding region (aa 320 to 433) (IcsA$_{i330a}$, IcsA$_{i330b}$, IcsA$_{i342}$, IcsA$_{i346}$, and IcsA$_{i381}$), within polar localization region 2 (aa 507 to 620) (IcsA$_{i532}$ and IcsA$_{i563}$), or within or adjacent to the putative autochaperone domain (aa 634 to 735) (IcsA$_{i633}$, IcsA$_{i643}$, IcsA$_{i677}$, and IcsA$_{i716}$). The remaining strains had intermediate phenotypes, exhibiting a WT frequency of plaque formation but forming plaques that varied in size compared to the control. Strains expressing the mutants IcsA$_{i56}$, IcsA$_{i595}$, and IcsA$_{i598}$ formed plaques that were smaller in diameter than those of bacteria expressing IcsA$_{WT}$ (30%, 51%, and 27% smaller, respectively). Additionally, while strains expressing IcsA$_{i193}$, IcsA$_{i288}$, IcsA$_{i312}$, and IcsA$_{i502}$ were unable to form plaques, they did form small foci of dead HeLa cells that were not observed for *S. flexneri* Δ*icsA*, suggesting that the mutants IcsA$_{i193}$, IcsA$_{i288}$, IcsA$_{i312}$, and IcsA$_{i502}$ still retained a limited capacity to promote intercellular spread (Table 2).

Effect of linker insertions on IcsA function in N-WASP recruitment and F-actin comet tail formation. To further investigate the molecular basis for the defects in intercellular spreading exhibited by strains expressing IcsA$_i$ proteins, the ability of these strains to recruit host N-WASP and form F-actin comet tails was examined by IF microscopy using anti-N-WASP antibodies and FITC-phalloidin, respectively. Nineteen out of the 29 strains expressing IcsA$_i$ mutants were unable to either recruit N-WASP or form F-actin comet tails (Table 2). All of these strains had also been negative for plaque formation. This included strains expressing the mutant proteins IcsA$_{i185}$, IcsA$_{i219}$, IcsA$_{i226}$, IcsA$_{i230}$, IcsA$_{i244}$, IcsA$_{i248}$, IcsA$_{i268}$, IcsA$_{i271}$, and IcsA$_{i297}$, with insertions within the GRR region, strains expressing IcsA$_{i330a}$, IcsA$_{330b}$, IcsA$_{i342}$, IcsA$_{i346}$, and IcsA$_{i381}$, with linker insertions within the IcsB binding region, and strains expressing IcsA$_{i532}$ and IcsA$_{i563}$ with linker insertions within polar localization region 2.

Although a strain producing IcsA$_{i346}$ was unable to form F-actin comet tails, capping of the bacterial pole with F-actin was observed, despite undetectable N-WASP recruitment (Table 2). Also, while they were unable to form detectable plaques or foci, F-actin tail formation was seen at a very low frequency (in <10% of infected cells) for strains producing IcsA$_{i228}$, IcsA$_{i292}$ (which had insertions located in the GRR region), and IcsA$_{i633}$ (which had an insertion in the putative autochaperone region), and N-WASP recruitment could be detected only with the latter two mutants (Table 2). Strains producing IcsA$_{i595}$ and IcsA$_{i598}$ that had reduced levels of protein were readily able to recruit N-WASP (Table 2) and form F-actin comet tails (Fig. 5A).

Although *S. flexneri* strains expressing IcsA$_{i56}$, IcsA$_{i193}$, IcsA$_{i288}$, IcsA$_{i312}$, and IcsA$_{i502}$ formed reduced-size plaques, these mutants still displayed efficient N-WASP recruitment (Table 2) and F-actin comet tail formation (Fig. 5A). To reconcile these data, it was hypothesized that the frequency of tail formation of these strains may have been only slightly reduced, resulting in a decrease in intercellular spreading and plaque formation. Accordingly, F-actin comet tail formation was more rigorously quantitated (see Materials and Methods) in order to detect any small changes in F-actin tail formation frequency. The mutants IcsA$_{i598}$ and IcsA$_{i595}$ were not included in these studies since the low-level production of these mutant proteins would complicate interpretation of their phenotypes. Interestingly, for all strains tested, F-actin comet tail formation was found to occur at a frequency that was not statistically different from that with IcsA$_{WT}$, except for strains expressing IcsA$_{i288}$ ($P < 0.001$) and IcsA$_{i502}$ ($P < 0.05$) (Fig. 5B).

Effect of LPS Oag on F-actin comet tail formation and N-WASP recruitment by *S. flexneri* expressing IcsA mutants. We have previously shown that smooth-LPS (S-LPS) populations, possessing the Oag component, can mask IcsA function (31, 32). Therefore, it was of interest to determine if IcsA$_i$ mutants that were unable to recruit N-WASP in an S-LPS background could do so in an *S. flexneri* strain that has only "rough" LPS (R-LPS) populations that lack the Oag component. Furthermore, it was of interest to determine if expression of IcsA$_i$ mutants in this background would restore the ability of these IcsA$_i$ mutants to form F-actin comet tails. Sixteen IcsA$_i$ mutants (Table 2) that were either unable or had a reduced ability to recruit N-WASP and induce F-actin comet tails were expressed in an R-LPS *S. flexneri* Δ*icsA* Δ*rmlD* strain (RMA2043), and the intracellular behavior of each strain was examined by IF microscopy.

Remarkably, when either the IcsA$_{i185}$, IcsA$_{i226}$, IcsA$_{i532}$, or

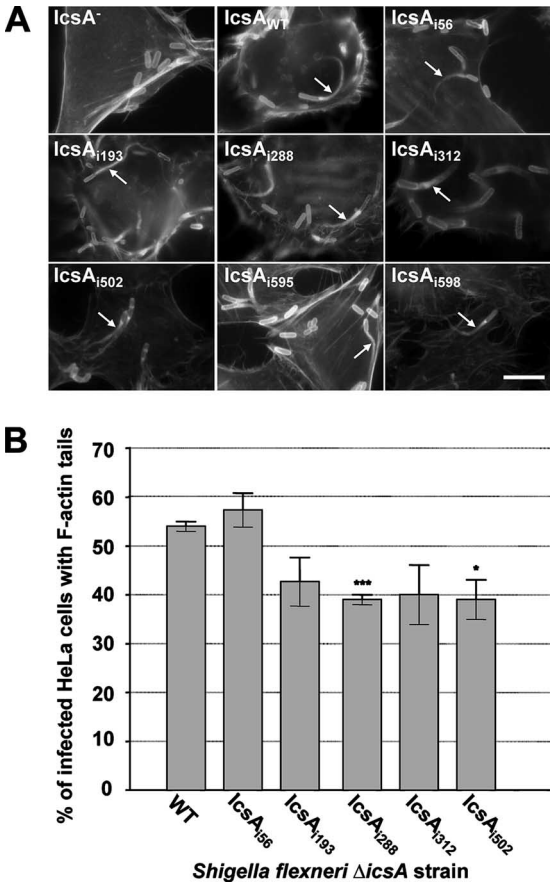

FIG. 5. F-actin comet tail formation by intracellular *S. flexneri* Δ*icsA* strains expressing $IcsA_{-i}$ mutants. (A) IF microscopy of F-actin tail formation by intracellular *S. flexneri* Δ*icsA* strain expressing $IcsA_{-i}$ mutants. HeLa cells infected with *S. flexneri* were labeled with anti-LPS antibodies and Alexa 594-conjugated donkey antirabbit antibodies, and F-actin was labeled with FITC-phalloidin. Arrows indicate F-actin tail formation. Strains were assessed in three independent experiments. Scale bar = 10 μm. (B) Frequency of F-actin tail formation by *S. flexneri* Δ*icsA* strains expressing $IcsA_{-i}$ mutants. HeLa cells were infected with *S. flexneri* strains and examined by IF microscopy as detailed in Materials and Methods. The frequency of F-actin tail formation was determined by observing the percentage of infected HeLa cells ($n = 100$) that had at least 1 F-actin tail. Data represent means ± standard errors. *, $P < 0.05$; ***, $P < 0.001$ (determined by Student's unpaired two-tailed t test). Data are from three independent experiments.

$IcsA_{i563}$ mutants were expressed in an R-LPS *S. flexneri* Δ*icsA* Δ*rmlD* strain, F-actin comet tail formation and N-WASP recruitment were observed (Fig. 6; Table 2), albeit at a lower frequency (10 to 20% of infected cells contained F-actin comet tails) than with the *S. flexneri* Δ*icsA* Δ*rmlD* strain expressing $IcsA_{WT}$ (RMA2107; Table 1) (54% of infected cells had F-actin comet tails). For $IcsA_{i228}$, N-WASP recruitment could not be detected when this mutant was expressed in an S-LPS *S. flexneri* Δ*icsA* strain, despite this strain occasionally forming F-actin comet tails (Table 2). However, when $IcsA_{i228}$ was expressed in the R-LPS *S. flexneri* Δ*icsA* Δ*rmlD* strain, N-WASP recruitment could be detected and F-actin comet tail formation occurred more frequently (albeit still at a lower frequency than with the *S. flexneri* Δ*icsA* Δ*rmlD* strain expressing $IcsA_{WT}$). Additionally, for the *S. flexneri* Δ*icsA* Δ*rmlD* strain expressing $IcsA_{i271}$, N-WASP recruitment could be detected, albeit faintly (Table 2). For the remaining R-LPS strains that were investigated, N-WASP recruitment and F-actin comet tail formation could not be detected (Table 2).

The identification of $IcsA_i$ proteins that were able to recruit N-WASP and induce F-actin comet tails in an R-LPS background but not in the presence of S-LPS was interesting. Based on this finding, it was hypothesized that previously reported IcsA deletion mutants (49–51) would also be subject to masking by LPS Oag, perhaps to even a greater extent since these IcsA constructs possessed large deletions ranging in size from 188 aa to 404 aa. Suzuki et al. (51) reported that $IcsA_{\Delta 103–320}$, $IcsA_{\Delta 508–730}$, and $IcsA_{\Delta 103–507}$ were unable to induce F-actin comet tail formation when expressed by an S-LPS *S. flexneri* Δ*icsA* strain, although $IcsA_{\Delta 508–730}$ did induce F-actin accumulation. Furthermore, the latter mutant was reported to recruit N-WASP, while the others did not (49, 50). Hence, plasmids encoding $IcsA_{\Delta 103–320}$ (pD10-*virG*1), $IcsA_{\Delta 508–730}$ (pD10-*virG*3), and $IcsA_{\Delta 103–507}$ (pD10-*virG*4) were expressed in an R-LPS *S. flexneri* Δ*icsA* Δ*rmlD* strain (RMA2043), and N-WASP recruitment and F-actin comet tail formation were examined. As reported previously for S-LPS strains, when these proteins were expressed in an R-LPS background, none of the IcsA deletion mutant proteins were able to induce F-actin tail formation (Fig. 7; Table 3). The N-WASP recruitment and circumferential accumulation of F-actin observed when $IcsA_{\Delta 508-730}$ was expressed in an S-LPS *S. flexneri* background were also observed when this construct was expressed in an R-LPS background (Fig. 7; Table 3). Surprisingly, though, the other two mutants, $IcsA_{\Delta 103-320}$ and $IcsA_{\Delta 103-507}$, also exhibited a low level of N-WASP recruitment when expressed in an R-LPS *S. flexneri* strain (Fig. 7; Table 3). These results indicate that these deletion mutations retain some residual N-WASP recruitment activity that is masked in an S-LPS background.

DISCUSSION

The IcsA (VirG) protein of *S. flexneri* is essential for virulence, and through its interaction with host N-WASP, it is able to initiate F-actin comet tail formation, leading to bacterial ABM and intercellular spreading throughout the colonic epithelium (2, 17, 18, 24, 52). The aim of our study was to refine our understanding of the IcsA structure-function relationship using pentapeptide mutagenesis, since previous studies have for the most part utilized either large deletion mutations or expression of small fragments of IcsA to identify functional domains. Linker insertion mutagenesis is an effective tool for examining structure-function relationships and has been used successfully for other AT proteins (7, 12, 22). There is the potential for such insertions to impact on the overall structure of the target protein, and the effects may not be strictly localized to the sight of the insertion. Therefore, we have attempted to address this issue by assessing the protease accessibility of mutants as a probe for major alterations of protein conformation. Nonetheless, our data obtained using the linker insertion mutagenesis approach are consistent with those of previous studies and have additionally allowed us to identify novel functional regions within the passenger domain.

Of the 47 $IcsA_i$ mutants that were created in this study, 6

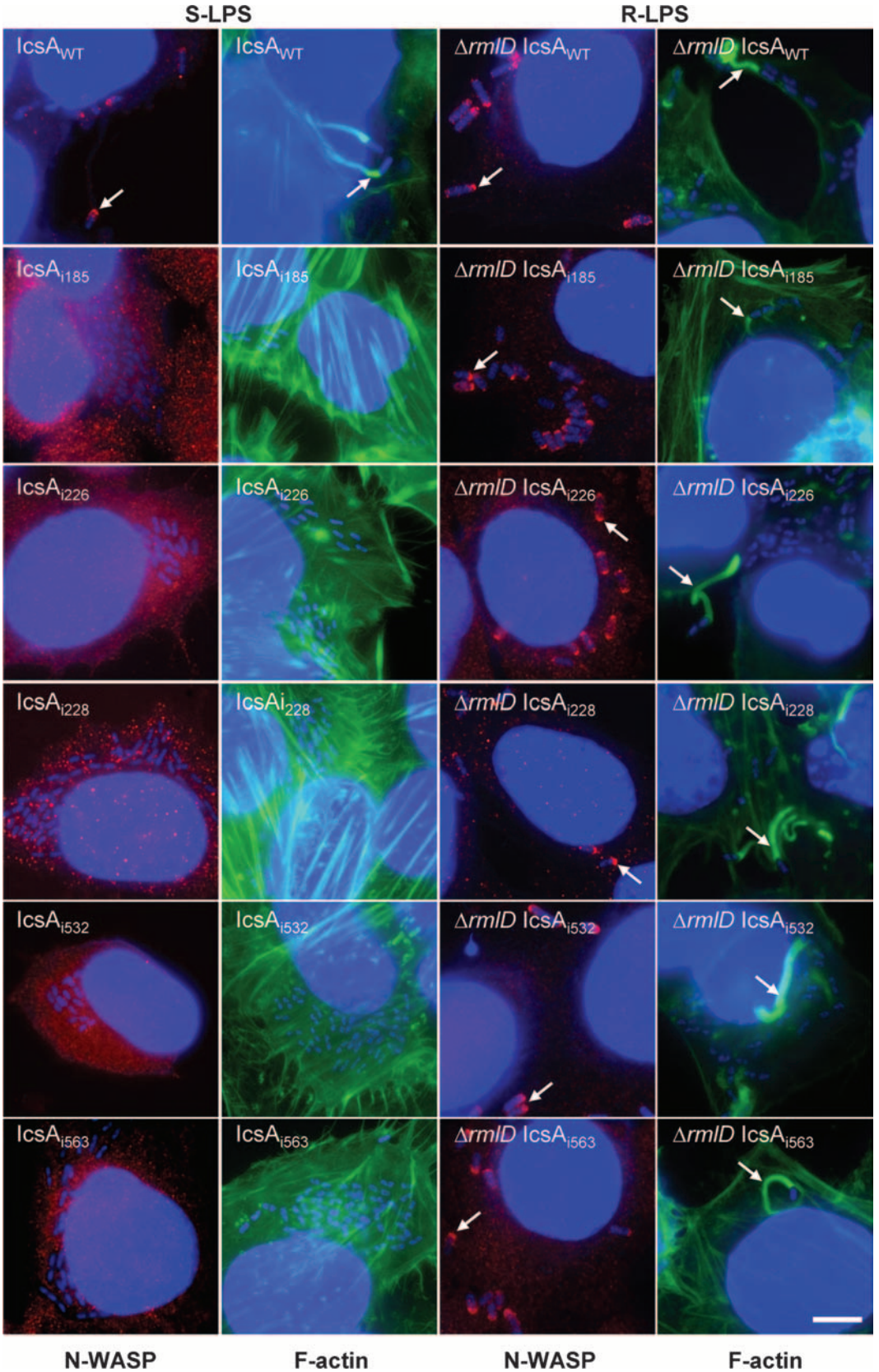

FIG. 6. N-WASP recruitment and F-actin comet tail formation by intracellular *S. flexneri* strains expressing the IcsA$_i$ proteins with either smooth or rough LPS. IF microscopy of F-actin tail formation and N-WASP recruitment by intracellular *S. flexneri* strains expressing IcsA$_{-i}$ mutants. HeLa cells were infected with *S.* the *flexneri* Δ*icsA* (S-LPS) or *S. flexneri* Δ*icsA* Δ*rmlD* (R-LPS) strain expressing IcsA$_i$ proteins and formalin fixed. Bacteria were labeled with DAPI (blue), F-actin was labeled with FITC-phalloidin (green), and N-WASP was labeled with anti-N-WASP and Alex 594-conjugated donkey antirabbit antibodies (red) as detailed in Materials and Methods. Arrows indicate F-actin tail formation and N-WASP recruitment. Strains were assessed in two independent experiments. Bar = 10 μm.

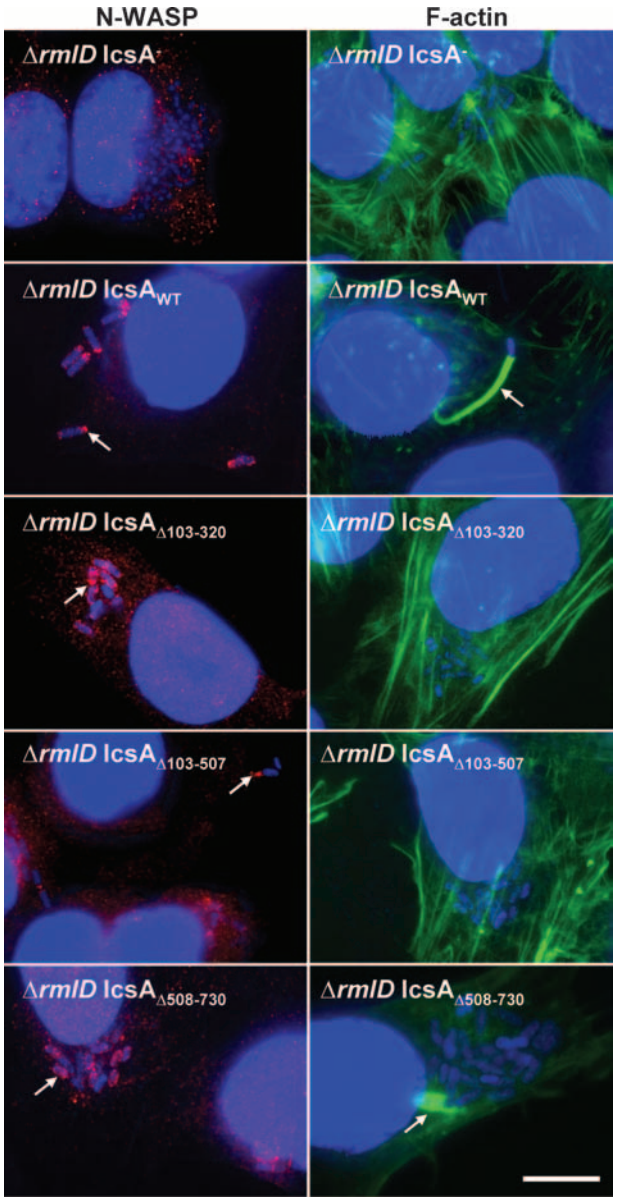

FIG. 7. N-WASP recruitment and F-actin comet tail formation by intracellular *S. flexneri* strains expressing IcsA deletion mutant proteins with either smooth or rough LPS. IF microscopy of F-actin tail formation and N-WASP recruitment by intracellular *S. flexneri* strains expressing IcsA$_{Δ}$ mutants. HeLa cells were infected with *S. flexneri* Δ*icsA* (S-LPS) or *S. flexneri* Δ*icsA* Δ*rmlD* (R-LPS) strains expressing IcsA deletion mutant proteins and formalin fixed. Bacteria were labeled with DAPI (blue), F-actin was labeled with FITC-phalloidin (green), and N-WASP was labeled with anti-N-WASP and Alex 594-conjugated donkey antirabbit antibodies (red) as detailed in Materials and Methods. Arrows indicate F-actin tail formation or N-WASP recruitment. Strains were assessed in two independent experiments. Bar = 10 μm.

proteins (IcsA$_{i595}$, IcsA$_{i598}$, IcsA$_{i633}$, IcsA$_{i643}$, IcsA$_{i677}$, and IcsA$_{i716}$) demonstrated reduced production of both cell-associated and secreted forms in *S. flexneri*. However, production of IcsA$_{i595}$, IcsA$_{i598}$, and IcsA$_{i633}$ was restored to WT levels when they were expressed in *E. coli* UT5600 (Δ*ompP* Δ*ompT*), consistent with the hypothesis that these proteins may be sensitive to degradation by endogenous OM proteases. Production of IcsA$_{i643}$, IcsA$_{i677}$, and IcsA$_{i716}$ was still greatly reduced in *E. coli* UT5600, suggesting sensitivity to degradation by periplasmic proteases, such as DegP. Indeed, DegP has been implicated in IcsA export (20, 43, 44). Additionally, all six mutants demonstrated increased sensitivity to trypsin. A change in protease accessibility of these mutants implies a conformational alteration compared to IcsA$_{WT}$. Oliver et al. (39) have previously described a putative intramolecular chaperone region of the passenger domain conserved between several AT proteins, including IcsA (aa 634 to 735). In the *B. pertussis* AT protein, BrkA, deletion of this autochaperone region (aa 601 to 692) made the protein susceptible to degradation by OM proteases and trypsin. Similarly, this has also been shown for homologous regions within other autotransporter proteins, SSP, Pet, and AIDA-1 (3, 12, 38). The role of this region in IcsA biogenesis had not been previously investigated. Our study provides the first experimental evidence implicating this region of IcsA as a putative autochaperone domain. Owing to the associated production defect, it was not possible to determine the contribution of this region to N-WASP recruitment and F-actin comet tail formation.

Two regions of the passenger domain (aa 1 to 104 and aa 507 to 620) have previously been attributed to polar localization of IcsA (9, 51). We have identified two mutants, IcsA$_{i532}$ and IcsA$_{i563}$, with altered IcsA localization on the surface of *S. flexneri*. Both of these mutants possessed linker insertions within polar localization region 2 (aa 507 to 620); three mutants (IcsA$_{i56}$, IcsA$_{i81}$, and IcsA$_{i87}$) that possessed linker insertions within polar localization region 1 (aa 1 to 104) were all polarly distributed. Our data suggest that polar targeting region 1 is not able to compensate for mutational alterations in

TABLE 3. F-actin comet tail formation and N-WASP recruitment by R-LPS *S. flexneri* Δ*icsA* Δ*rmlD* strains expressing IcsA$_i$ mutants

Protein expressed	Phenotype of *S. flexneri* Δ*icsA* Δ*rmlD* strain[a]	
	F-actin tail formation	N-WASP recruitment
IcsA$_{WT}$	+++	+++
IcsA$_{i185}$	++	++
IcsA$_{i219}$	−	−
IcsA$_{i226}$	++	++
IcsA$_{i228}$	++	++
IcsA$_{i244}$	−	−
IcsA$_{i248}$	−	−
IcsA$_{i268}$	−	−
IcsA$_{i271}$	−	+
IcsA$_{i297}$	−	−
IcsA$_{i330a}$	−	−
IcsA$_{i330b}$	−	−
IcsA$_{i342}$	−	−
IcsA$_{i346}$	−	+/−
IcsA$_{i381}$	−	−
IcsA$_{i532}$	++	++
IcsA$_{i563}$	++	++
IcsA$_{Δ103–320}$	−	+
IcsA$_{Δ508–730}$	+/−	+
IcsA$_{Δ103–507}$	−	+

[a] +++, WT N-WASP recruitment/F-actin comet tail formation; ++, 50 to 90% reduction in N-WASP recruitment/F-actin tail formation relative to IcsA$_{WT}$; +, >90% reduction in N-WASP recruitment/F-actin tail formation; +/−, F-actin capping; −, N-WASP/F-actin tail formation not detected. Two independent experiments (n = 20) were carried out.

region 2. These results refute the significance of polar targeting region 1, which has previously been reported to be targeted to the pole independently of polar targeting region 2 (9).

Another significant finding from our study was that the interaction between N-WASP and some $IcsA_i$ and $IcsA_\Delta$ proteins inside host cells was influenced by LPS Oag. By assessing protein function in an R-LPS background, we were able to account for masking of mutant proteins by LPS Oag when interpreting the resulting phenotypes. The mutants $IcsA_{i185}$, $IcsA_{i226}$, $IcsA_{i532}$, and $IcsA_{i563}$ were unable to recruit N-WASP and induce F-actin comet tails when expressed in S-LPS *S. flexneri* Δ*icsA* strains. However, these mutants were able to recruit N-WASP and form F-actin tails in an R-LPS *S. flexneri* background (albeit at a lower frequency than R-LPS *S. flexneri* expressing $IcsA_{WT}$). Additionally, the $IcsA_{\Delta 103–320}$ and $IcsA_{\Delta 103–507}$ deletion mutants examined in our study, although unable to recruit N-WASP when expressed by S-LPS *S. flexneri*, were able to recruit N-WASP when expressed by R-LPS *S. flexneri* strains. Hence, mutations in IcsA that abolish N-WASP recruitment do not necessarily indicate mutational alteration of N-WASP binding regions of IcsA but may be due to LPS-Oag-dependent interference in IcsA–N-WASP interactions, possibly due to conformational alterations or truncation of mutant proteins.

In our study, the ability of mutants to facilitate F-actin comet tail formation correlated with N-WASP recruitment. However, we identified *icsA*$_i$ mutants that had proficient F-actin comet tail formation but were defective in intercellular spread. The molecular basis of this defect is currently under investigation, but these findings highlight the need for intercellular spreading to be directly assessed when determining the relative contributions of various host and bacterial factors to the process of ABM.

The region spanning aa 103 to 433 of IcsA has previously been shown to be adequate for N-WASP binding, as established by in vitro pull-down assays (49, 50), and IcsA aa 53 to 508 are sufficient to induce actin polymerization during in vitro assays (17). Therefore, it was not surprising that most of the linker insertions within this region disrupted IcsA function in N-WASP recruitment and ABM. Fifteen $IcsA_i$ mutants had linker insertions within the GRR region (aa 140 to 307), and nine of these mutant proteins ($IcsA_{i185}$, $IcsA_{i219}$, $IcsA_{i226}$, $IcsA_{i230}$, $IcsA_{i244}$, $IcsA_{i248}$, $IcsA_{i268}$, $IcsA_{i271}$, and $IcsA_{i297}$) were to unable induce N-WASP recruitment and F-actin comet tail formation when expressed by *S. flexneri* in infected cells. Although deletion of aa 104 to 226 has been reported to abolish F-actin comet tail formation (51), this had not been correlated with N-WASP recruitment. Data from our study confirm the involvement of this region in N-WASP recruitment. Five mutants ($IcsA_{i330a}$, $IcsA_{330b}$, $IcsA_{i342}$, $IcsA_{i346}$, and $IcsA_{i381}$) with linker insertions within the IcsB binding region (aa 320 to 433) were also unable either to form plaques or F-actin comet tails or to recruit N-WASP when expressed by *S. flexneri*. These *icsA*$_i$ mutants differ phenotypically from the *icsB* mutants from previous studies (36, 37), which were unable to form plaques in tissue culture monolayers but were able to form F-actin tails and exhibit actin-based motility at a frequency similar to that of the WT up to 3 h postinfection (37).

Significantly, we observed that an R-LPS *S. flexneri* strain expressing $IcsA_{\Delta 103–507}$ exhibited a low level of N-WASP recruitment. Since this deletion mutation removes both the GRR region and the IcsB regions, it suggests that an additional region(s) was involved in N-WASP recruitment. Deletion of aa 508 to 730 of IcsA has previously been shown to affect F-actin comet tail formation (51). However, the $IcsA_{\Delta 508–730}$ mutant also displayed aberrant localization on the surface of bacteria, complicating the interpretation of this mutant's phenotype (51). Indeed, the authors of that paper suggested that the defect in F-actin comet tail formation resulted from nonpolar localization of IcsA. Our study has identified two mutants, $IcsA_{i532}$ and $IcsA_{i563}$, which are also nonpolarly expressed on the surface of *S. flexneri* and are unable to induce F-actin comet tail formation in S-LPS strains (like $IcsA_{\Delta 508–730}$). However, F-actin comet tail formation was restored, albeit at a low frequency, when these mutants were expressed in an R-LPS strain. The same was not observed for $IcsA_{\Delta 508–730}$, which was unable to induce F-actin comet tail formation in R-LPS strains. The latter indicates that an additional defect occurs as a result of deleting this region that is independent of the effect on IcsA polarity.

The results of our study suggest a previously unidentified region of IcsA (aa 508 to 730) is important for N-WASP recruitment and F-actin comet tail formation, and this warrants further investigation. We propose a model to reconcile this data, in which multiple regions of IcsA are required for N-WASP recruitment. Our model is supported by the demonstration that WASP homology domain 1 and the Cdc42/Rac interactive binding domain of N-WASP are independently recruited to *S. flexneri* inside N-WASP-deficient cell lines or HeLa cells (25, 30). The determination of the structure of IcsA and IcsA in complex with N-WASP (with and without LPS Oag) would clearly assist our understanding of the binding process.

ACKNOWLEDGMENTS

We thank Hiroaki Miki for the kind gifts of N-WASP antisera and His-tagged and glutathione *S*-transferase-tagged N-WASP constructs and Chihiro Sasakawa for *virG* deletion constructs. We gratefully acknowledge Luisa Van Den Bosch and Lisa Clark for technical assistance and Marcin Grabowicz for critically reading the manuscript.

This work was supported by a project grant from the National Health and Medical Research Council of Australia awarded to R.M. K.L.M. was the recipient of a Faculty of Science Postgraduate Scholarship from the University of Adelaide.

REFERENCES

1. **Baker, S., J. Gunn, and R. Morona.** 1999. The *Salmonella typhi* melittin resistance gene *pqaB* affects intracellular growth in PMA-differentiated U937 cells, polymyxin B resistance and lipopolysaccharide. Microbiology **145:**367–378.
2. **Bernardini, M. L., J. Mounier, H. d'Hauteville, M. Coquis-Rondon, and P. J. Sansonetti.** 1989. Identification of *icsA*, a plasmid locus of *Shigella flexneri* that governs bacterial intra- and intercellular spread through interaction with F-actin. Proc. Natl. Acad. Sci. USA **86:**3867–3871.
3. **Berthiaume, F., N. Rutherford, and M. Mourez.** 2007. Mutations affecting the biogenesis of the AIDA-I autotransporter. Res. Microbiol. **158:**348–354.
4. **Brahmbhatt, H. N., A. A. Lindberg, and K. N. Timmis.** 1992. *Shigella* lipopolysaccharide: structure, genetics, and vaccine development. Curr. Top. Microbiol. Immunol. **180:**45–64.
5. **Brandon, L. D., N. Goehring, A. Janakiraman, A. W. Yan, T. Wu, J. Beckwith, and M. B. Goldberg.** 2003. IcsA, a polarly localized autotransporter with an atypical signal peptide, uses the Sec apparatus for secretion, although the Sec apparatus is circumferentially distributed. Mol. Microbiol. **50:**45–60.
6. **Brandon, L. D., and M. B. Goldberg.** 2001. Periplasmic transit and disulfide bond formation of the autotransported *Shigella* protein IcsA. J. Bacteriol. **183:**951–958.
7. **Charbonneau, M.-E., and M. Mourez.** 2007. Functional organization of the

autotransporter adhesin involved in diffuse adherence. J. Bacteriol. **189:** 9020–9029.
8. **Charles, M., J. Magdalena, J. A. Theriot, and M. B. Goldberg.** 1999. Functional analysis of a rickettsial OmpA homology domain of *Shigella flexneri* IcsA. J. Bacteriol. **181:**869–878.
9. **Charles, M., M. Perez, J. H. Kobil, and M. B. Goldberg.** 2001. Polar targeting of *Shigella* virulence factor IcsA in *Enterobacteriacae* and *Vibrio*. Proc. Natl. Acad. Sci. USA **98:**9871–9876.
10. **Cossart, P.** 2000. Actin-based motility of pathogens: the Arp2/3 complex is a central player. Cell. Microbiol. **2:**195–205.
11. **d'Hauteville, H., R. Dufourcq Lagelouse, F. Nato, and P. Sansonetti.** 1996. Lack of cleavage of IcsA in *Shigella flexneri* causes aberrant movement and allows demonstration of a cross-reactive eukaryotic protein. Infect. Immun. **64:**511–517.
12. **Dutta, P. R., B. Q. Sui, and J. P. Nataro.** 2003. Structure-function analysis of the enteroaggregative *Escherichia coli* plasmid-encoded toxin autotransporter using scanning linker mutagenesis. J. Biol. Chem. **278:**39912–39920.
13. **Egile, C., H. d'Hauteville, C. Parsot, and P. J. Sansonetti.** 1997. SopA, the outer membrane protease responsible for polar localization of IcsA in *Shigella flexneri*. Mol. Microbiol. **23:**1063–1073.
14. **Frischknecht, F., S. Cudmore, V. Moreau, I. Reckmann, S. Rottger, and M. Way.** 1999. Tyrosine phosphorylation is required for actin-based motility of *Vaccinia* but not *Listeria* or *Shigella*. Curr. Biol. **9:**89–92.
15. **Fukuda, I., T. Suzuki, H. Munakata, N. Hayashi, E. Katayama, M. Yoshikawa, and C. Sasakawa.** 1995. Cleavage of *Shigella* surface protein VirG occurs at a specific site, but the secretion is not essential for intracellular spreading. J. Bacteriol. **177:**1719–1726.
16. **Fukuoka, M., H. Miki, and T. Takenawa.** 1997. Identification of N-WASP homologs in human and rat brain. Gene **196:**43–48.
17. **Goldberg, M. B.** 2001. Actin-based motility of intracellular microbial pathogens. Microbiol. Mol. Biol. Rev. **65:**595–626.
18. **Goldberg, M. B., O. Barzu, C. Parsot, and P. J. Sansonetti.** 1993. Unipolar localization and ATPase activity of IcsA, a *Shigella flexneri* protein involved in intracellular movement. J. Bacteriol. **175:**2189–2196.
19. **Henderson, I. R., F. Navarro-Garcia, M. Desvaux, R. C. Fernandez, and D. Ala'Aldeen.** 2004. Type V protein secretion pathway: the autotransporter story. Microbiol. Mol. Biol. Rev. **68:**692–744.
20. **Jain, S., and M. B. Goldberg.** 2007. Requirement for YaeT in the outer membrane assembly of autotransporter proteins. J. Bacteriol. **189:**5393–5398.
21. **Jann, K., and B. Jann.** 1987. Polysaccharide antigens of *Escherichia coli*. Rev. Infect. Dis. **9:**S517–S526.
22. **Klemm, P., L. Hjerrild, M. Gjermansen, and M. A. Schembri.** 2004. Structure-function analysis of the self-recognizing antigen 43 autotransporter protein from *Escherichia coli*. Mol. Microbiol. **51:**283–296.
23. **Kotloff, K. L., F. Noriega, G. A. Losonsky, M. B. Sztein, S. S. Wasserman, J. P. Nataro, and M. M. Levine.** 1996. Safety, immunogenicity, and transmissibility in humans of CVD 1203, a live oral *Shigella flexneri* 2a vaccine candidate attenuated by deletions in *aroA* and *virG*. Infect. Immun. **64:**4542–4548.
24. **Lett, M. C., C. Sasakawa, N. Okada, T. Sakai, S. Makino, M. Yamada, K. Komatsu, and M. Yoshikawa.** 1989. *virG*, a plasmid-coded virulence gene of *Shigella flexneri*: identification of the VirG protein and determination of the complete coding sequence. J. Bacteriol. **171:**353–359.
25. **Lommel, S., S. Benesch, K. Rottner, T. Franz, J. Wehland, and R. Kuhn.** 2001. Actin pedestal formation by enteropathogenic *Escherichia coli* and intracellular motility of *Shigella flexneri* are abolished in N-WASP-defective cells. EMBO Rep. **2:**850–857.
26. **Lugtenberg, B., J. Meijers, R. Peters, P. van der Hoek, and L. van Alphen.** 1975. Electrophoretic resolution of the "major outer membrane protein" of *Escherichia coli* K12 into four bands. FEBS Lett. **58:**254–258.
27. **Makino, S., C. Sasakawa, K. Kamata, T. Kurata, and M. Yoshikawa.** 1986. A genetic determinant required for continuous reinfection of adjacent cells on large plasmid in *S. flexneri* 2a. Cell **46:**551–555.
28. **Miki, H., and T. Takenawa.** 2003. Regulation of actin dynamics by WASP family proteins. J. Biochem. **134:**309–313.
29. **Monack, D. M., and J. A. Theriot.** 2001. Actin-based motility is sufficient for bacterial membrane protrusion formation and host cell uptake. Cell. Microbiol. **3:**633–647.
30. **Moreau, V., F. Frischknecht, I. Reckmann, R. Vincentelli, G. Rabut, D. Stewart, and M. Way.** 2000. A complex of N-WASP and WIP integrates signalling cascades that lead to actin polymerization. Nat. Cell Biol. **2:**441–448.
31. **Morona, R., C. Daniels, and L. Van Den Bosch.** 2003. Genetic modulation of *Shigella flexneri* 2a lipopolysaccharide O antigen modal chain length reveals that it has been optimized for virulence. Microbiology **149:**925–939.
32. **Morona, R., and L. Van Den Bosch.** 2003. Lipopolysaccharide O antigen chains mask IcsA (VirG) in *Shigella flexneri*. FEMS Microbiol. Lett. **221:** 173–180.
33. **Morona, R., and L. Van Den Bosch.** 2003. Multicopy *icsA* is able to suppress the virulence defect caused by the *wzzSF* mutation in *Shigella flexneri*. FEMS Microbiol. Lett. **221:**213–219.
34. **Morona, R., L. Van Den Bosch, and P. Manning.** 1995. Molecular, genetic, and topological characterization of O-antigen chain length regulation in *Shigella flexneri*. J. Bacteriol. **177:**1059–1068.
35. **Oaks, E. V., M. E. Wingfield, and S. B. Formal.** 1985. Plaque formation by virulent *Shigella flexneri*. Infect. Immun. **48:**124–129.
36. **Ogawa, M., T. Suzuki, I. Tatsuno, H. Abe, and C. Sasakawa.** 2003. IcsB, secreted via the type III secretion system, is chaperoned by IpgA and required at the post-invasion stage of *Shigella* pathogenicity. Mol. Microbiol. **48:**913–931.
37. **Ogawa, M., T. Yoshimori, T. Suzuki, H. Sagara, N. Mizushima, and C. Sasakawa.** 2005. Escape of Intracellular *Shigella* from Autophagy. Science **307:**727–731.
38. **Ohnishi, Y., M. Nishiyama, S. Horinouchi, and T. Beppu.** 1994. Involvement of the COOH-terminal pro-sequence of *Serratia marcescens* serine protease in the folding of the mature enzyme. J. Biol. Chem. **269:**32800–32806.
39. **Oliver, D. C., G. Huang, E. Nodel, S. Pleasance, and R. C. Fernandez.** 2003. A conserved region within the *Bordetella pertussis* autotransporter BrkA is necessary for folding of its passenger domain. Mol. Microbiol. **47:**1367–1383.
40. **Pallen, M. J., R. R. Chaudhuri, and I. R. Henderson.** 2003. Genomic analysis of secretion systems. Curr. Opin. Microbiol. **6:**519–527.
41. **Pantaloni, D., C. L. Clainche, and M.-F. Carlier.** 2001. Mechanism of actin-based motility. Science **292:**1502–1506.
42. **Philpott, D. J., J. D. Edgeworth, and P. J. Sansonetti.** 2000. The pathogenesis of *Shigella flexneri* infection: lessons from *in vitro* and *in vivo* studies. Philos. Trans. R. Soc. Lond. B Biol. Sci. **355:**575–586.
43. **Purdy, G. E., C. R. Fisher, and S. M. Payne.** 2007. IcsA surface presentation in *Shigella flexneri* requires the periplasmic chaperones DegP, Skp, and SurA. J. Bacteriol. **189:**5566–5573.
44. **Purdy, G. E., M. Hong, and S. M. Payne.** 2002. *Shigella flexneri* DegP facilitates IcsA surface expression and is required for efficient intercellular spread. Infect. Immun. **70:**6355–6364.
45. **Sansonetti, P. J., J. Arondel, A. Fontaine, H. d'Hauteville, and M. L. Bernardini.** 1991. *OmpB* (osmo-regulation) and *icsA* (cell-to-cell spread) mutants of *Shigella flexneri*: vaccine candidates and probes to study the pathogenesis of shigellosis. Vaccine **9:**416–422.
46. **Shere, K. D., S. Sallustio, A. Manessis, T. G. D'Aversa, and M. B. Goldberg.** 1997. Disruption of IcsP, the major *Shigella* protease that cleaves IcsA, accelerates actin-based motility. Mol. Microbiol. **25:**451–462.
47. **Steinhauer, J., R. Agha, T. Pham, A. W. Varga, and M. B. Goldberg.** 1999. The unipolar *Shigella* surface protein IcsA is targeted directly to the bacterial old pole: IcsP cleavage of IcsA occurs over the entire bacterial surface. Mol. Microbiol. **32:**367–377.
48. **Suzuki, T., M.-C. Lett, and C. Sasakawa.** 1995. Extracellular transport of VirG protein in *Shigella*. J. Biol. Chem. **270:**30874–30880.
49. **Suzuki, T., H. Miki, T. Takenawa, and C. Sasakawa.** 1998. Neural Wiskott-Aldrich syndrome protein is implicated in the actin-based motility of *Shigella flexneri*. EMBO J. **17:**2767–2776.
50. **Suzuki, T., H. Mimuro, S. Suetsugu, H. Miki, T. Takenawa, and C. Sasakawa.** 2002. Neural Wiskott-Aldrich syndrome protein (N-WASP) is the specific ligand for *Shigella* VirG among the WASP family and determines the host cell type allowing actin-based spreading. Cell. Microbiol. **4:**223–233.
51. **Suzuki, T., S. Saga, and C. Sasakawa.** 1996. Functional analysis of *Shigella* VirG domains essential for interaction with vinculin and actin-based motility. J. Biol. Chem. **271:**21878–21885.
52. **Suzuki, T., and C. Sasakawa.** 2001. Molecular basis of the intracellular spreading of *Shigella*. Infect. Immun. **69:**5959–5966.
53. **Van den Bosch, L., P. A. Manning, and R. Morona.** 1997. Regulation of O-antigen chain length is required for *Shigella flexneri* virulence. Mol. Microbiol. **23:**765–775.
54. **Van den Bosch, L., and R. Morona.** 2003. The actin-based motility defect of a *Shigella flexneri rmlD* rough LPS mutant is not due to loss of IcsA polarity. Microb. Pathog. **35:**11–18.
55. **Yarar, D., W. To, A. Abo, and M. D. Welch.** 1999. The Wiskott-Aldrich syndrome protein directs actin-based motility by stimulating actin nucleation with the Arp2/3 complex. Curr. Biol. **9:**555–559.